Measuring the Radial Field of Muon g-2

GEM Internship Report at Fermilab

Fatima Rodriguez

Supervisors: Saskia Charity and Brendan Kiburg

July 2022- August 2022

Abstract

In the measurement of the electric dipole moment (EDM), a leading systematic error is the presence of radial magnetic fields which tilts the precession plane and is indistinguishable from a true EDM. The average radial magnetic field can be determined by studying the muon beam distribution and its vertical components. To minimize this systematic uncertainty in EDM analysis, we re-designed a platform that will allow us to attach a Hall probe and directly measure the radial magnetic field as a function of azimuth.

1 Introduction

Muon g-2 aims to measure the anomalous magnetic moment of a muon

$$a_\mu = \frac{g_\mu - 2}{2} \tag{1}$$

where g_μ is defined as the g-factor that relates the magnetic dipole moment of a muon to its spin.

$$\vec{\mu} = g_\mu(\frac{q}{2m_\mu})\vec{s} \tag{2}$$

In other words, the magnetic moment of the muon characterizes how it interacts under an external magnetic field. The g-factor can be derived by using the Dirac equation, which yield $g = 2$ for spin-1/2 particles; however, due to experimental results for the g-factor of a proton, $g_p \approx 5.6$, the magnetic moment is now expressed by

$$\mu = (1 + a)\frac{q\hbar}{2m} \tag{3}$$

where a is defined by Eq[1].Ultimately, the anomalous magnetic moment of a particle can be calculated with high precision using the standard model, which returns $a_\mu(SM) = 16591810(43) \times 10^{-11}$ for a muon.

In 2001, Brookhaven National Laboratory obtained a result using a 50-foot diameter superconducting storage ring (SR) of $a_\mu(BNL) = 116592080(63) \times 10^{-11}$, which is larger than $a_\mu(SM)$ by 3.7σ. Due to this discrepancy, Fermilab performed their own Muon g-2 experiment using the same 1.45 T superconducting SR from BNL, but with 2.5 times improved magnetic field intrinsic uniformity, detailed beam storage simulations, and improved calorimetry and field metrology. Fermilab released results in 2021 within a precision of 0.46 ppm of $a_\mu(FNAL) = 116592040(54) \times 10^{-11}$.

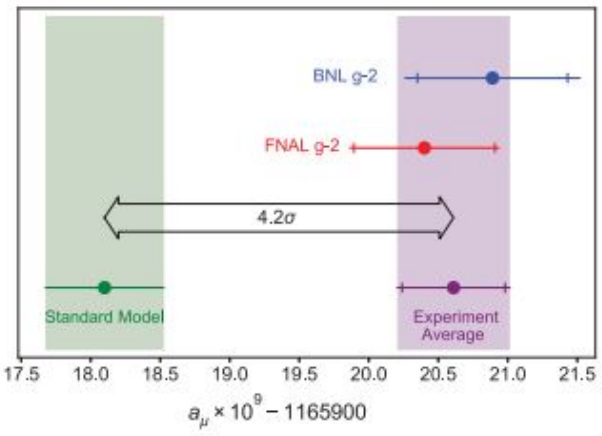

Figure 1: Experimental results of a_μ obtained by BNL and Fermilab in comparison to the standard model prediction. The experimental value greater than 4σ suggests underlying physics that diverge from the standard model! figure obtained by [1].

Muon g-2 also performs studies on the electric dipole moment (EDM) of a muon, defined by

$$\vec{d} = \eta(\frac{q}{2mc})\vec{s} \tag{4}$$

where c is the speed of light in a vacuum, η is a dimensionless quantity relating the EDM and the spin, analogous to the g-factor. An EDM measurement

defines the separation of positive and negative electrical charges within a system. This violates both parity (P) and time-reversal (T) symmetries; therefore, detecting a non-zero EDM in Muon g-2 would place a constraint in CP-violation (charge symmetry and parity symmetry), indicating new physics that diverge from the standard model. However, due to the presence of a radial magnetic field in the Muon g-2 environment, the effects of a non-zero EDM on the muon spin precession plane is indistinguishable to the effects caused by a radial field, as shown in Figure 3.

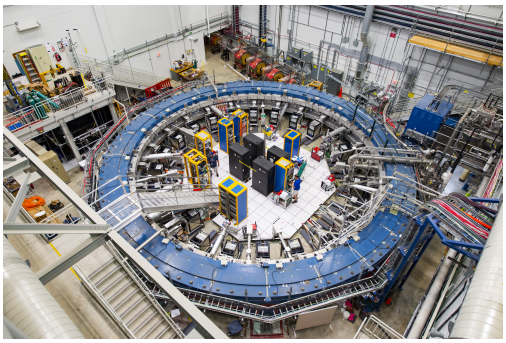

Figure 2: Picture of Muon g-2 at Fermilab, taken by Reidar Hahn (2002).

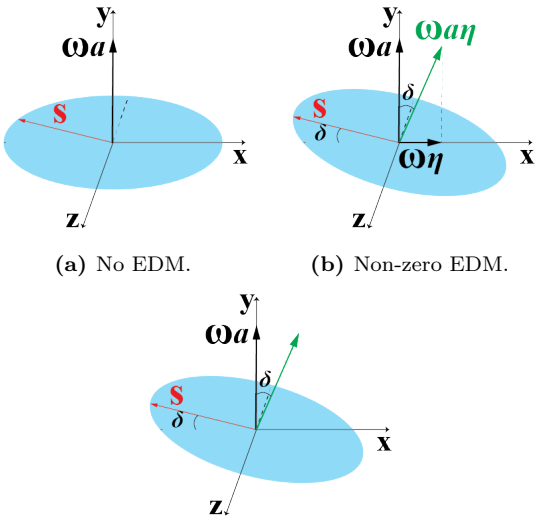

(a) No EDM.

(b) Non-zero EDM.

(c) Under a radial magnetic field.

Figure 3: Muon spin precession planes under no EDM, non-zero EDM, and radial field. Under a non-zero EDM, the muon would experience torque which introduces an additional spin precession frequency $\omega_{a\eta}$. This experienced torque also causes the plane to tilt radially, as it would under a radial magnetic field.

In this study, I contribute towards obtaining a measurement of the radial magnetic field to minimize systematic uncertainty in EDM analysis for Run 5. This is done by first analyzing its effect on the beam position (Section 2) and by designing a new apparatus that will allow us to directly measure the radial field from inside the vacuum chamber (Section 3). Conclusions and remarks are noted in Section 4.

2 Beam Method

The presence of a radial field affects the vertical position of the beam as shown in the Eq 5:

$$< y >= \frac{< B_r >}{V}, < B_r >=< B_r^a > + < B_r^b > \quad (5)$$

where $< y >$ is the average vertical position of the beam, $< B_r >$ is the average radial field, $< B_r^a >$ is an applied radial field, $< B_r^b >$ is a background radial field, and V is the electro-static quadrupole (ESQ) voltage [3]. By performing scans at different ESQ voltage settings and surface correction coil (SCC) currents, we can measure how the vertical position of the beam varies through those settings and find an optimal SCC setting to minimize $< B_r^b >$.

2.1 Surface Correction Coils (SCC)

There are 72 pole pieces strategically placed in the SR that drives the overall field strength [2]. The SCC, which consist of 100 individually powered concentric coils, sit on upper and lower surface of each pole piece. By driving specific current distributions to the SCC, variations of the field can by minimized across the beam aperture. Therefore, we can apply a range of applied radial fields, $< B_r^a >$, using the SCC.

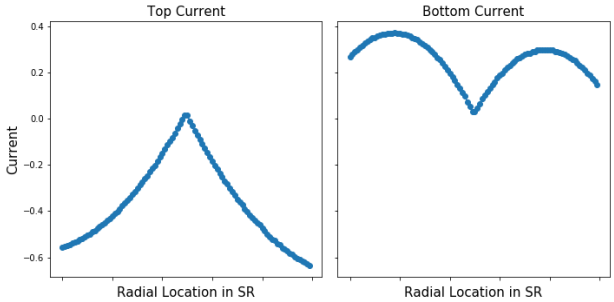

Figure 4: Plot of top and bottom current for run number 9030. Coil 0 is radially outwards and coil 100 is radially inwards.

2.2 Measuring $< y >$ Around the SR

The vertical position of the beam can be determined using data from the calorimeters. Each calorimeter is composed of 9×6 array of PbF_2 crystals and a silicon photomultiplier. Figure 5 is a representation of what each calorimeter views.

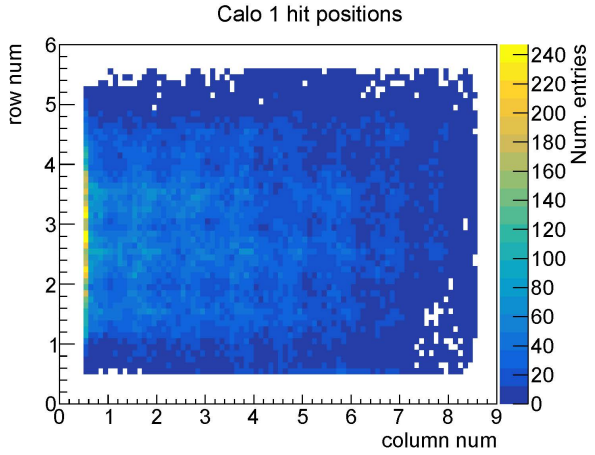

Figure 5: Azimuthal view of decay positron positions, detected by calorimeter 1. Plot created by Saskia Charity (2022).

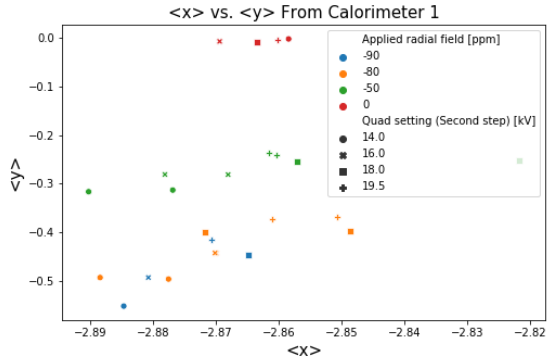

Figure 6: Average vertical position for each quad and radial field setting against the average horizontal position. The $< y >$ tends to increase as the applied field from the SCC decrease. It is also interesting to note how the ESQ settings effect $< x >$.

The average vertical position of the beam at each calorimeter location can be obtained by averaging the row numbers of each calorimeter. Similarly, we can do the same to the column numbers to obtain an averaged horizontal position. This process can be repeated at different SCC and ESQ settings to analyze how the vertical position changes around the SR, as shown in Figure 6.

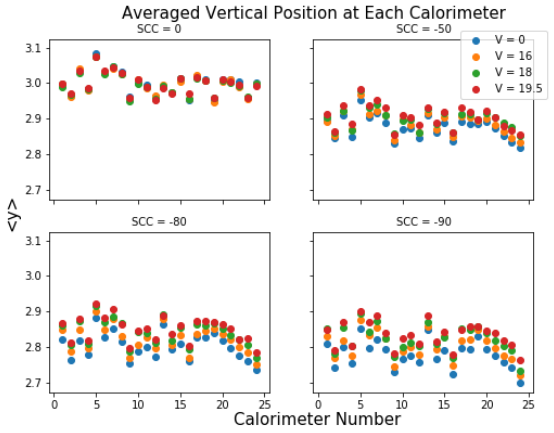

Figure 7: Average vertical positions of the beam at each calorimeter and at different applied radial fields of 0, -50, -80, and -90. Here we can see how an applied radial field causes real effects to the vertical position of the beam despite voltage settings. These plots were created with Run 5 data.

2.3 Measuring $< y >$ Over All Calorimeters

By averaging the localized $< y >$ for each SCC and ESQ setting, we can obtain an overall averaged vertical position of the beam. These results are shown in Figure 8.

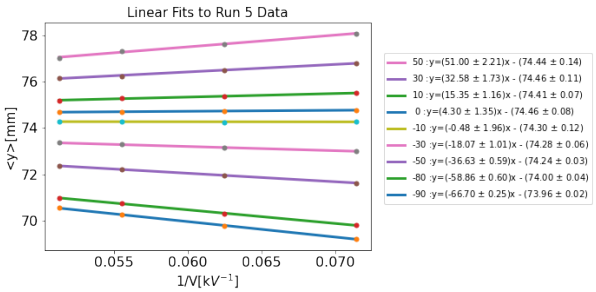

Figure 8: Averaged vertical position of the muon bean for each SCC setting over ESQ voltage and their linear fits. This plot confirms the linear relationship between radial field and vertical beam position. Data points were obtained by Dominika Vasilkova.

2.4 Measuring $< B_r^b >$

The background radial field is due to the radial components of any unintentional magnetic fields present in the Muon g-2 environment. We can measure $< B_r >$ by finding the point where $< B_r >= 0$ such that $< B_r^a >= - < B_r^b >$ from Eq.5. This would

be equivalent to the SCC setting that returns a zero gradient to a linear fit. Therefore, by plotting the gradients for each linear fit in Figure 8 against their corresponding applied field, we can create a secondary linear fit to obtain the applied field at zero gradient. This procedure was performed for two separate ranges of applied fields to check the validity of the data below applied fields of -50 ppm.

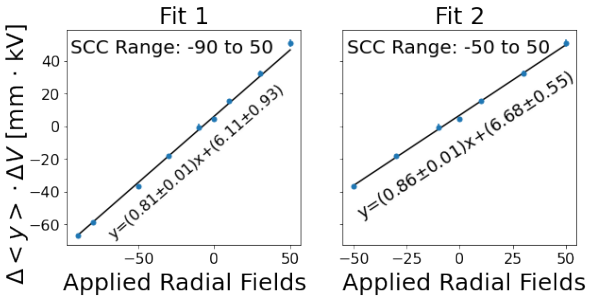

Figure 9: Gradient vs. applied radial field. Optimal applied radial field for zero gradient is 7.53 ± 1.15 ppm and 7.74 ± 0.65 ppm, for Fit 1 and Fit 2 respectively.

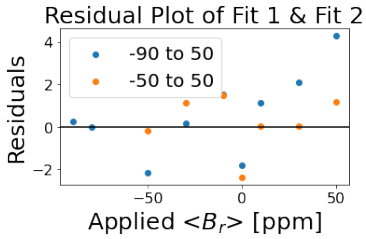

Figure 10: Residual plot for both fits from Figure 8.

As shown in Figure 9, the residual plot of both fits show that a range of -50 to 50 ppm is best suited for a linear fit, hence showing that we are losing muons for lower SCC settings. The resulting $< B_r^b >$ from this analysis is 7.74 ± 0.65 ppm.

3 Measuring the Radial Field

We can directly measure the radial magnetic field by using a Hall probe. The Hall probe will detect the magnitude of the magnetic field using the Hall effect, such that the output voltage of the Hall probe will be directly proportional to the strength of the magnetic field at different radial and azimuthal locations. Measurements were last performed in 2019 by Rachel Osofsky [4] using the platform shown in Figure 11.

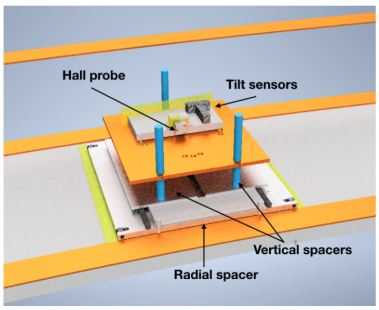

Figure 11: The Hall probe platform used for radial field measurements in 2019. This design allowed measurements to be taken at different heights and radial positions.

To best measure the radial field that the muon experience, we decided to relocate the platform inside the vacuum chamber in place of the trolley garage shown in Figure 12. The trolley garage is a rail area where the trolley that maps the magnetic field is parked when not being used. This location is additionally best because the trolley garage can be easily detached without causing damage to additional parts within the chamber. However, this relocation would require a re-design of the Hall platform in order to match the dimensions inside the vacuum chamber, while still maintaining its up-down and radial mobility.

(a) Vacuum chamber with the trolley garage installed.

(b) Vacuum chamber without the trolley garage.

Figure 12: Pictures of the vacuum chamber with and without the trolley garage installed.

3.1 Designing a New Platform

The following conditions were considered during the re-design process of the Hall platform: 1) It must fit within the dimensions of the trolley garage area in the vacuum chamber. 2) It needs azimuthal, radial, and up-down mobility to allow several measurements to be taken. 3) The Hall probe must be aligned to the beam's radial center (280"R). 4) To save time and resources, it's best to re-use as many parts possible from the last design. An evolution of how the final design was created can be shown in Appendix A.

3.1.1 Determining Dimensional Constraints

The garage trolley is used as a reference for the new dimensions of the Hall platform, which are 16.47" azimuthally and 5.27" in height. We have more freedom radially inward with the restriction of keeping the probe at the beam's center.

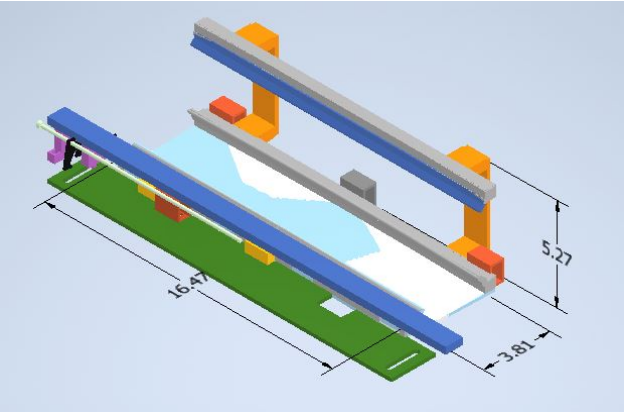

Figure 13: A CAD model of the garage trolley. The new platform will be designed in reference to the garage trolley dimensions.

may delay are time in taking measurements. Additionally, there is some down time to consider when placing the probe at different azimuthal or radial locations. Lifting the top apparatus up and aligning with the drilled holes may cause the Hall probe/tilt sensor to settle. Changing the bottom platform to a sliding mechanism may be ideal.

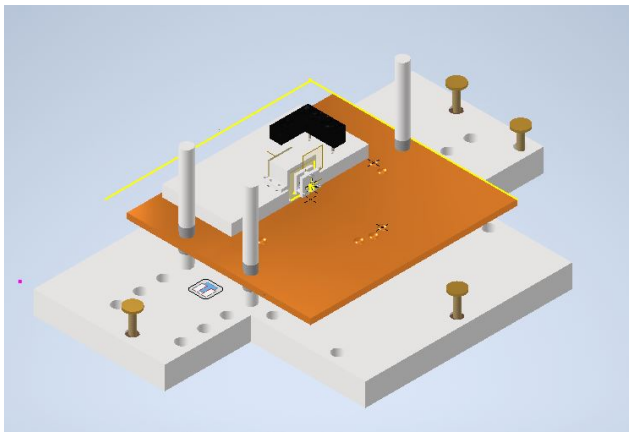

Figure 14: Final version of the platform design created with Inventor.

3.2 New Platform Design

The new platform shown in Figure 14 was designed such that it's azimuthal length is equivalent to the trolley garage; hence, making it easier to slide into place with the offset of the beam center to the back wall already accounted for. The drilled holes in the bottom platform allow for the top portion of the platform to move to 7 different azimuthal and radial locations. The height of the platform can also be adjusted using the threaded center of the rods before placing on the bottom platform. The top orange platform is a re-used part that maintains the probe aligned to the center, even when rotating radially. Rotating the top gray platform where the Hall probe is mounted on will allow us to take longitudinal measurements as well.Both the orange platform and the top gray platform are re-usable parts from the 2019 design; however, the orange platform had to be trimmed 1" from its side to keep the probe at the center beam. Full drawings with dimensions can be found in Appendix B.

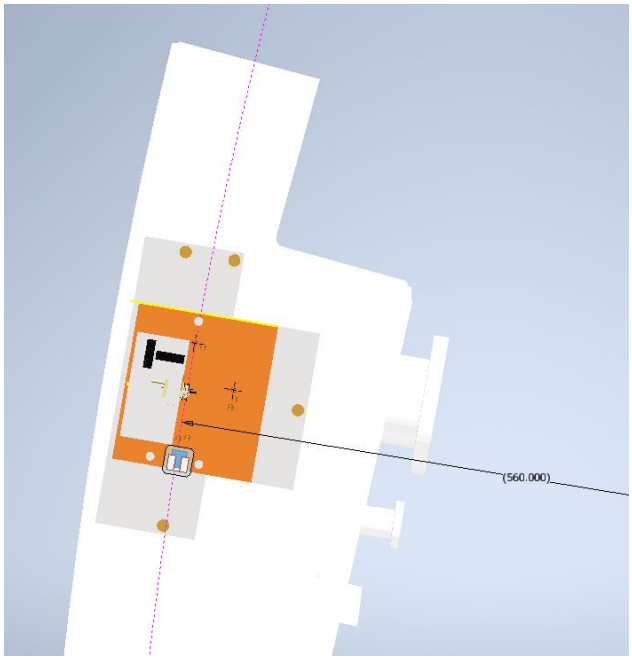

Figure 15: Inventor model of the new platform on a model of the inflector chamber, where the dashed line represents the beam center at 280"R. This process was used to check the new platform dimensions.

3.2.1 Future Improvements

Although, some parts from the 2019 platform were maintained, the bottom platform and centered-threaded rods would have to be sent to be built, which

4 Conclusions

The beam method accurately describes how that vertical position of the beam proportionally relates to an applied radial field. My contributions in reproducing the beam method analysis in Python allowed confirmation on a radial background measurement of 7.74 ± 0.65. This result will allow us to adjust the SCC settings and minimize radial background detection.

Once the new platform measurements and design are confirmed, the new platform will obtain measurements with higher accuracy than measurements done in 2019 because of its new location inside the vacuum chamber. These new radial field measurements would ultimately be applied to minimize systematic uncertainty in EDM analysis.

5 Acknowledgements

Thank you to my advisors, Saskia Charity and Brendan Kiburg for their kind support in this project. Thank you, Dominika Vasilkova for your valuable input in the beam method analysis. This project could also not have been possible without my Fermilab mentors, Carrie McGivern and Donovan Tooke. Thank you for providing all kinds of support throughout my Fermilab internship experience. Thank you Cool-Group-2 for your wonderful feedback and support. Finally, thank you to the Muon g-2 Collaboration for welcoming me into this project!

Appendices

Appendix A: Platform Design Evolution

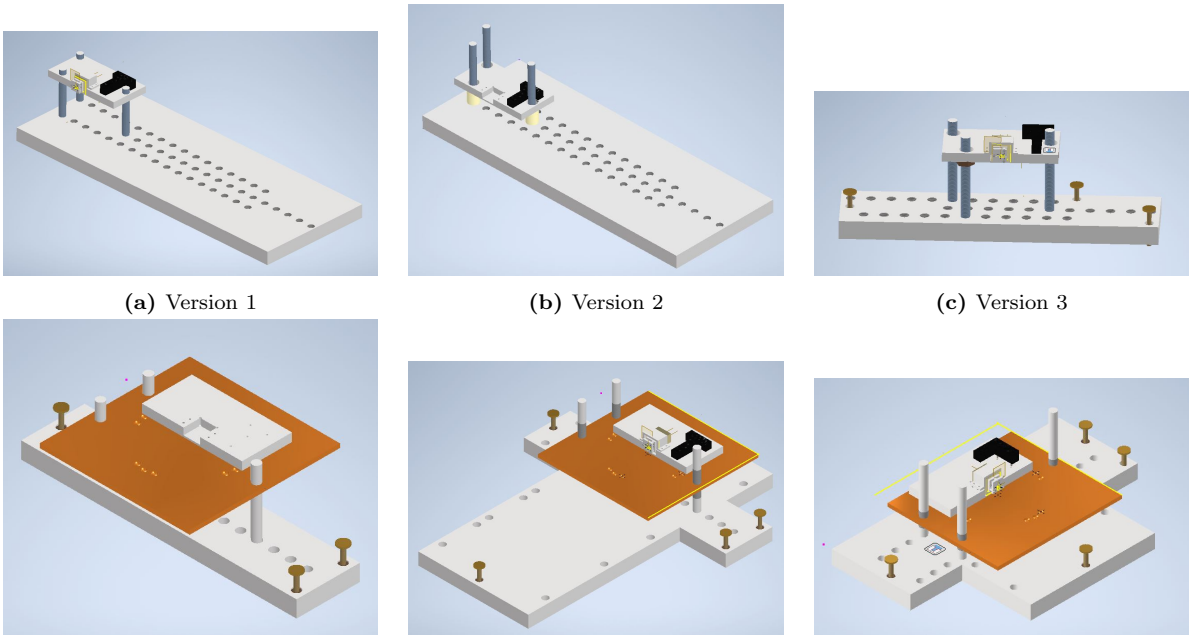

(a) Version 1 **(b)** Version 2 **(c)** Version 3

(d) Version 4 **(e)** Version 5 **(f)** Version 6

Figure 16: In Versions 1-3 I prioritized measuring only the radial field at different heights and azimuthal location. In Version 4, I realized that the hall probe was not centered to the garage rail so I decided to add the top orange platform from 2019. Not only would the probe be aligned due to the markings on the orange platform, but we would also be able to radially turn the probe for longitudinal measurements. In Version 5, the bottom platform is radially extended inward and outward. Due to the outward constraint to the back wall, the final design only extends radially inward and prioritizes the probe staying at the center of the beam.

Appendix B: Final Platform

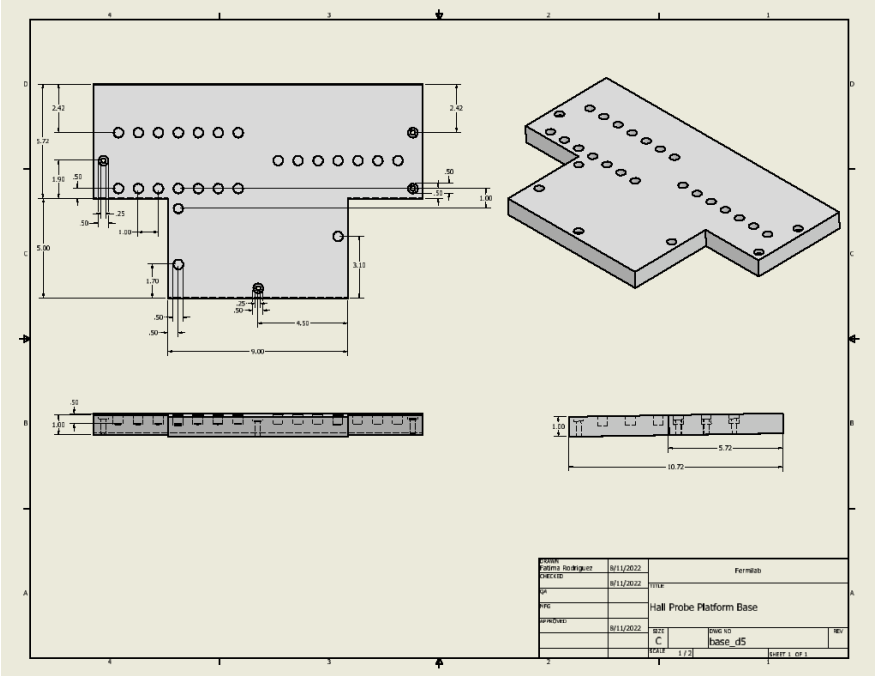

Figure 17: The base of the final platform design. This was designed to be the same azimuthal dimension as the garage trolley. It obtains 32 drilled holes of .5" depth for 8 different azimuthal and radial locations.

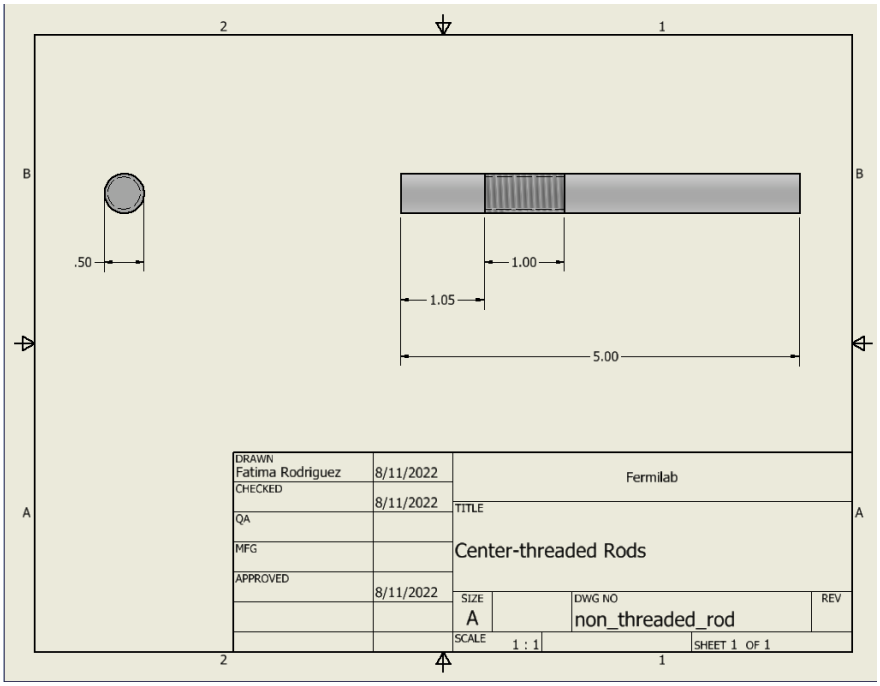

Figure 18: The centered-threaded rods that connect the top alignment platform with the base. It is specifically threaded at an offset from the base of 1.05" in order to keep the probe near the center of the beam (located at 2.795" from the bottom of the vacuum chamber). The threaded region only expands .5" from the center of the beam.

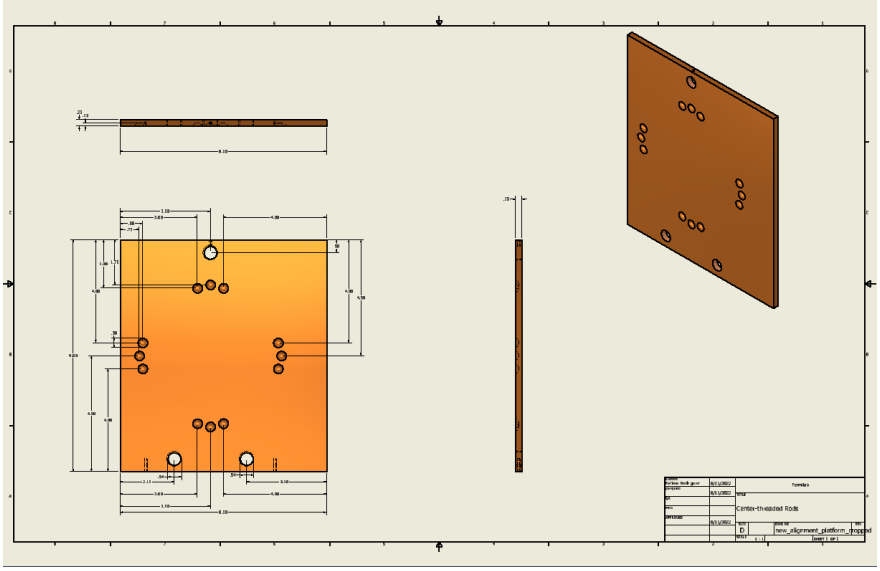

Figure 19: Top alignment platform that is re-used from previous platform design in 2019. Previously it was a 9x9" platform, but due to limitations from the vacuum chamber's back wall, 1" is trimmed from the left side, resulting in a 9x8" platform. New holes would have to be drill the location specified.

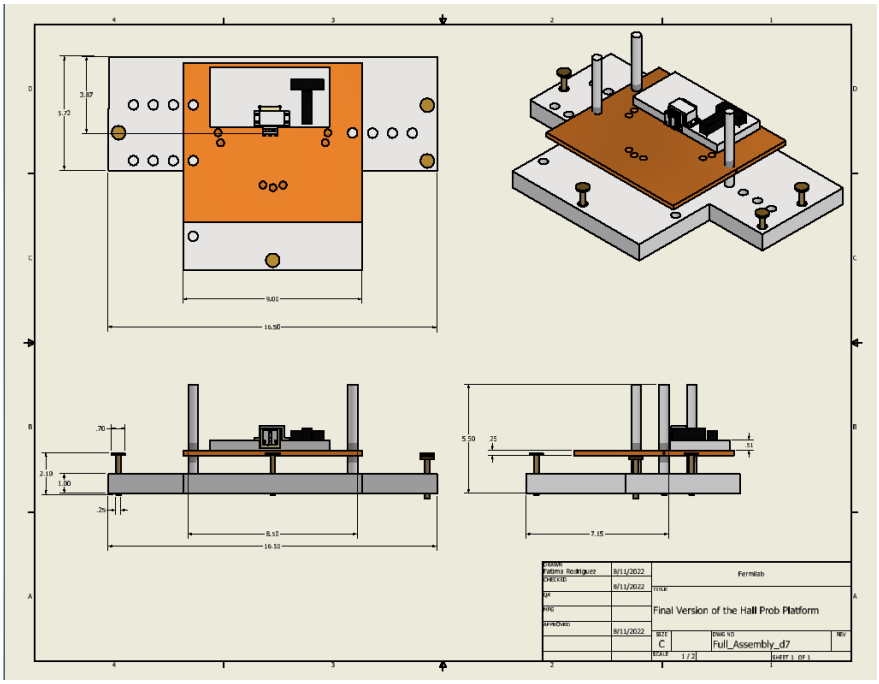

Figure 20: Drawing of the full platform assembly. The top gray platform that the Hall probe is mounted on stays unchanged.

References

[1] B. Abi et al. "Measurement of the Positive Muon Anomalous Magnetic Moment to 0.46 ppm". In: *Phys. Rev. Lett.* 126 (14 Apr. 2021), p. 141801. DOI: 10.1103/PhysRevLett.126.141801. URL: https://link.aps.org/doi/10.1103/PhysRevLett.126.141801.

[2] T. Albahri et al. “Magnetic-field measurement and analysis for the Muon mml:math xmlns:mml=”http://www.w3.org/199 /mml:momml:mn2/mml:mn/mml:mrow/mml:math Experiment at Fermilab”. In: *Physical Review A* 103.4 (Apr. 2021). DOI: 10.1103/physreva.103.042208. URL: https://doi.org/10.1103%2Fphysreva.103.042208.

[3] Sam Grant. “Radial magnetic field measurements for an EDM search.” E989 note. 2022.

[4] Rachel Osofsky. “Magnetic field determination for run 1 of the Fermilab Muon G - 2 experiment”. PhD thesis.